

Dynamic-Range Enhancement for a Microwave Photonic Link Based on a Polarization Modulator

Xiang Chen, *Student Member, IEEE*, Wangzhe Li, *Member, IEEE*, and Jianping Yao, *Fellow, IEEE*

Abstract—A microwave photonic link (MPL) with an increased spurious-free dynamic range (SFDR) using a polarization modulator is proposed and experimentally demonstrated. The fundamental concept of the proposed approach to increase the SFDR is to reduce the third-order intermodulation distortion (IMD3) and to improve the modulation efficiency by partial carrier suppression, which is realized here by producing two channels of intensity-modulated signals with one having only the upper sidebands and the other having the optical carrier that is partially suppressed and the upper sidebands using two optical filters. If the optical powers into the two channels are kept identical, the combination of the two signals at a photodetector will fully cancel the IMD3 terms. In addition, the modulation efficiency is optimized due to the partial carrier suppression, which also leads to an increased SFDR. The proposed MPL is theoretically studied and experimentally demonstrated. An SFDR of 123.48 dB · Hz^{2/3} at a noise floor of −166 dBm/Hz is achieved, which is 15 dB higher than that of a regular intensity-modulation and direct-detection MPL.

Index Terms—Microwave photonic link (MPL), microwave photonics, optoelectronics, spurious-free dynamic range (SFDR).

I. INTRODUCTION

MICROWAVE photonic links (MPLs) with the ability to transmit microwave signals with a much wider bandwidth and lower loss over conventional coaxial analog links have been extensively studied over the last few years [1], [2]. An MPL is usually implemented based on intensity modulation and direct detection (IM/DD) using a Mach–Zehnder modulator (MZM) and a photodetector (PD). However, the inherent nonlinear modulation function of an MZM makes an IM/DD MPL have a small dynamic range. For many applications, such as broadband wireless access, and antenna remoting, an MPL with a high dynamic range is needed. To increase the dynamic range, several techniques have been proposed, including those implemented in the electrical domain and the optical domain. For example, in the electrical domain, pre-distortion techniques are used, such as those using an electrical circuit with an arcsine transfer function [3] and a feedback circuit to send the inverted intermodulation distortions to the RF input of the MPL

[4]. However, linearization techniques based on electrical circuits have a key limitation: small bandwidth. The bandwidth can be significantly increased if linearization is implemented in the optical domain. Numerous optical techniques have been proposed, including low biasing an MZM to partially suppress the optical carrier [5], an MZM operating at the opposite slopes of the transfer functions for two different wavelengths [6], and parallel operation of a pair of MZMs or polarization modulators (PolMs) [7]–[9]. The major disadvantage of the approach by low biasing an MZM [5] is that the second-order harmonic distortions and the second-order intermodulation distortion (IMD2) will be generated because of the increased nonlinearity when low biasing the MZM. The main idea behind the optical linearization methods in [6]–[9] is to have a main modulation path and an auxiliary modulation path, to generate two complementary third-order intermodulation distortion (IMD3) terms from the two paths. These distortions will be summed at a PD and be fully cancelled. Since two MZMs or PolMs, two laser sources or a pair of balanced PDs are used, the systems are more complicated and costly.

We have recently proposed two simplified schemes using a single PolM [10], [11] to operate equivalently as an MPL with two modulators. In [10], the MPL has a structure to allow the PolM to function as two equivalent MZMs operating at the opposite slopes. The IMD3 terms from the two channels will be combined destructively and be cancelled through utilizing a phase-shifted fiber Bragg grating (PS-FBG) as an optical notch filter to suppress partially the optical carrier of one channel. In an ideal situation, the notch of the optical notch filter should have an ultra-narrow width. For practical implementation, however, the notch has a finite width; some optical components close to the optical carrier are also removed, which may cause the IMD3 terms to fail to be completely suppressed. In addition, large second-order harmonic distortions and the IMD2 may also be generated because of the suppression of the optical carrier. Furthermore, in the theoretical analysis in [10], higher order optical sidebands were ignored, thus the distortions due to the higher order optical sidebands were not considered, which would affect the accuracy of the theoretical analysis. To avoid using an optical notch filter, which may remove optical components close to the optical carrier, in [11] we proposed an MPL in which a PolM was bidirectionally used in a Sagnac loop. The optical carrier in one channel is partially suppressed due to the destructive cancellation at the output of the Sagnac loop interferometer. Thus, optical components close to the optical carrier were not removed, and a higher spurious-free dynamic range (SFDR) could be achieved. The main limitation of the scheme in [11] is the relatively poor stability due to the

Manuscript received August 10, 2014; revised November 17, 2014 and April 06, 2015; accepted April 29, 2015. Date of publication May 15, 2015; date of current version July 01, 2015. This work was supported by the Natural Science and Engineering Research Council of Canada (NSERC).

The authors are with the Microwave Photonics Research Laboratory, School of Electrical Engineering and Computer Science, University of Ottawa, ON, Canada K1N 6N5 (e-mail: jpyao@eecs.uOttawa.ca).

Color versions of one or more of the figures in this paper are available online at <http://ieeexplore.ieee.org>.

Digital Object Identifier 10.1109/TMTT.2015.2430351

sensitive nature of an optical interferometer. Again, the cancellation of the IMD3 is at the cost of increasing second-order harmonic distortions and IMD2.

Therefore, there are two main techniques to improve the SFDR of an MPL, which are: 1) to reduce the IMD3 by pre-distortion [3], [4] or by using two optical paths to produce two identical, but complementary IMD3 terms [6]–[10] and 2) to partially suppress the optical carrier, to increase the modulation efficiency and the gain of the MPL [5]. To the best of our knowledge, no scheme has been proposed to utilize simultaneously the two techniques to increase the SFDR.

In this paper, we propose a new scheme to implement an MPL incorporating both techniques to further increase the SFDR. In the proposed MPL, two channels of intensity-modulated signals are generated using a PolM and two optical filters (OFs) with the upper channel having only the upper sidebands and the lower channel having the optical carrier and the upper sidebands. If the optical powers into the two channels are identical, the combination of the two signals at the PD will fully cancel the IMD3 terms. In addition, in the lower channel the biasing point of the modulator is lowered to partially suppress the optical carrier. If the optical power from the lower channel to the PD is maintained constant, the modulation efficiency is optimized, which would increase the gain of the link, and thus increasing the SFDR [5]. Compared with the scheme in [10], since the lower sidebands are totally suppressed, the proposed scheme has two advantages, which are: 1) the proposed MPL can tolerate the fiber chromatic dispersion and 2) the second-order harmonic distortions and the IMD2 will not be increased at the output of the PD although the optical carrier is suppressed. In addition, all the optical components contributing to the IMD3 terms are considered so the theoretical analysis is more precise. Since the two techniques to increase the SFDR are applied simultaneously to the proposed MPL, an improvement in SFDR of more than 15 dB is achieved in the experiment, which is 7.15 dB more than that of the MPL using two optical paths to produce two complementary IMD3 terms reported by us in [10].

This paper is organized as follows. In Section II, a theoretical analysis about the proposed MPL with a reduced IMD3 and an enhanced SFDR is provided. The operation is compared with a conventional PolM-based intensity-modulated MPL. In Section III, an experiment is performed where the SFDR and the IMD3 for the proposed MPL are measured and compared with those of a conventional PolM-based intensity-modulated MPL. In Section IV, some discussions are provided and a conclusion is drawn in Section V.

II. PRINCIPLE OF OPERATION

Fig. 1(a) shows the schematic of the proposed MPL. A linearly polarized light wave from a laser diode (LD) at λ_c is directed into a PolM via a polarization controller (PC₀). The PolM is a special phase modulator that supports phase modulation along the two principal axes with opposite phase modulation indices [12]. By tuning PC₀, the polarization direction of the incident light wave is adjusted to have an angle of 45° relative to one principal axis of the PolM. The phase-modulated signal from the PolM is split by a 3-dB coupler into two channels with identical powers. In the upper channel (Channel 1),

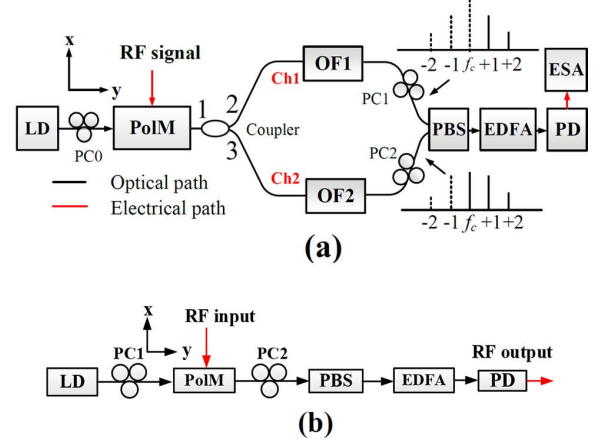


Fig. 1. (a) Schematic diagram of the proposed MPL. (b) Conventional PolM-based intensity-modulated MPL. Radio frequency: RF, laser diode: LD, polarization modulator: PolM, photodetector: PD, polarization controller: PC, polarization beam splitter: PBS, optical filter: OF, erbium-doped fiber amplifier: EDFA, electrical spectrum analyzer: ESA.

by a joint use of a PolM, a PC (PC₁), and a polarization beam splitter (PBS), an equivalent MZM is achieved, which is biased at the quadrature point by adjusting the static phase introduced by PC₁ [13]. An optical filter (OF1) is incorporated in the upper channel to filter out the optical carrier and the lower sidebands. In the lower channel (Channel 2), the PolM, another PC (PC₂), and the PBS again form an equivalent MZM, which is low biased by again adjusting the static phase introduced by the PC₂ [13]. The optical carrier and the upper sidebands are selected by a second optical filter (OF2). Finally, the two orthogonally polarized signals from the two channels are sent to a PD after amplification by an erbium-doped fiber amplifier (EDFA). The IMD3 terms are fully canceled at the output of the PD due to the destructive combination of the complementary distortion components.

First, we perform a two-tone analysis of a conventional PolM-based intensity-modulated MPL.

As can be seen in Fig. 1(b), a conventional PolM-based MPL consists of a PolM, two PCs (PC₁ and PC₂) before and after the PolM, and a PBS. The joint operation of the PolM, PC₂, and the PBS forms an equivalent MZM [12]. Mathematically, the optical fields at the output of the PolM along the principle axes (x and y) can be expressed as

$$\begin{bmatrix} E_x(t) \\ E_y(t) \end{bmatrix} = \frac{1}{\sqrt{2}} E_{\text{in}} \begin{bmatrix} e^{j(\omega_c t + \pi s_{\text{RF}}(t)/2V_\pi)} \\ e^{j(\omega_c t - \pi s_{\text{RF}}(t)/2V_\pi)} \end{bmatrix} \quad (1)$$

where E_{in} is the amplitude of the light wave at the input of the PolM, ω_c is the angular frequency of the optical carrier, $S_{\text{RF}}(t)$ is the input RF signal, and V_π is the half-wave voltage of the PolM. As can be seen, two complementarily phase-modulated signals are generated. Sending the two phase-modulated signals to the PBS, and if the principal axis of the PBS is aligned at 45° relative to one principle axis of the PolM by tuning PC₂, we then have

$$E(t) = \frac{\sqrt{2}}{2} [E_x(t)e^{j\phi/2} + E_y(t)e^{-j\phi/2}] \quad (2)$$

where ϕ is a static phase term introduced by the PC₂ placed before the PBS. The static phase term introduced by PC₂ can

be used to change the bias point of the equivalent MZM [12]. For a two-tone analysis, (2) can be rewritten as

$$\begin{aligned} E(t) &= E_c e^{j\{\beta[\cos(\Omega_1 t) + \cos(\Omega_2 t)]/2 + \phi/2\}} \\ &\quad + E_c e^{-j\{\beta[\cos(\Omega_1 t) + \cos(\Omega_2 t)]/2 + \phi/2\}} \\ E_c &= E_{in} \frac{e^{j\omega_c t}}{2} \\ \beta &= \frac{\pi V_s}{V_\pi} \end{aligned} \quad (3)$$

where β is the phase modulation index, Ω_1 and Ω_2 are the angular frequencies of two RF tones, and V_s is the amplitude of the two RF tones. Using the Jacobi–Auger expansions in (3), we can simplify (3), which is given by

$$\begin{aligned} E(t) &= E_c \sum_{p=-2}^{+2} \sum_{q=-2}^{+2} a_{p,q} e^{j(p\Omega_1 + q\Omega_2)t} \\ a_{p,q} &= j^{p+q} \cdot J_p J_q \left[e^{j\phi/2} + (-1)^{p+q} e^{-j\phi/2} \right] \end{aligned} \quad (4)$$

where $J_p = J_p(\beta/2)$ and $J_q = J_q(\beta/2) \cdot J_p(\cdot)$, $J_q(\cdot)$ are the Bessel functions of the first kind. According to [14], high-order terms (≥ 3) can be ignored, as their contributions are relatively small and can be neglected without loss of accuracy.

We then explain the operation of the proposed scheme shown in Fig. 1(a). In the upper channel, the only difference from the conventional PolM-based MPL shown in Fig. 1(b) is that an optical filter (OF1) is used to filter out the optical carrier and all the lower sidebands. If only the upper channel is connected to the PBS, when we set $\phi = -\pi/2$, which is a static phase term introduced by PC1 placed before the PBS, the equivalent MZM is thus biased at the quadrature point, and the optical field of the output signal from the PBS can be expressed by

$$E_1(t) = \frac{E_{C1} e^{j\omega_c t}}{2} \left\{ \begin{array}{l} \sqrt{2} J_{+1} J_0 [e^{j\Omega_2 t} + e^{j\Omega_1 t}] \\ \sqrt{2} J_{+2} J_{-1} [e^{j(2\Omega_1 - \Omega_2)t} + e^{j(2\Omega_2 - \Omega_1)t}] \\ -\sqrt{2} J_{+2} J_0 [e^{j2\Omega_2 t} + e^{j2\Omega_1 t}] \\ -\sqrt{2} J_{+1} J_{+1} e^{j(\Omega_2 + \Omega_1)t} \end{array} \right\} \quad (5)$$

where E_{C1} is the amplitude of the input light wave for the upper channel.

After the square-law detection at the PD, the generated photocurrent is given by

$$\begin{aligned} I_{ac1} &= \frac{\Re|E_1|^2}{2} \\ &\approx P_{in1} \Re \left\{ \begin{array}{l} -[J_{+1} J_0^2 J_{+2} + J_{+1}^3 J_0] \begin{bmatrix} \cos(\Omega_1 t) \\ +\cos(\Omega_2 t) \end{bmatrix} \\ -[J_{+1} J_0^2 J_{+2}] \begin{bmatrix} \cos((2\Omega_1 - \Omega_2)t) \\ +\cos((2\Omega_2 - \Omega_1)t) \end{bmatrix} \end{array} \right\} \end{aligned} \quad (6)$$

where \Re is the responsivity of the PD. $P_{in1} = E_{C1}^2/2$ is the input optical power for the upper channel. Note that (6) is obtained when only the main contributors to the fundamental and the IMD3 terms are taken into account.

Similarly, in the lower channel, an optical filter (OF2) is used to filter out the lower sidebands and partially suppress the optical carrier, leaving the upper sidebands unchanged. Assume a is the optical carrier power suppression index, defined as the ratio between the powers of the optical carrier before and after the OF2. When only the lower channel is connected to the PBS, the optical field of the output signal from the PBS can be expressed as (7), shown at the bottom of this page, where E_{C2} is the amplitude of the input light wave for the lower channel, and ϕ is a static phase term introduced by PC2 placed before the PBS, which determines the bias point of the equivalent MZM. In the proposed system, the equivalent MZM in the lower channel is low biased by tuning PC2. The photocurrent at the output of the PD is given by (8), shown at the bottom of this page, where $P_{in2} = E_{C2}^2/2$ is the input optical power. When the upper and the lower channels are both connected to the PBS, at the output of the PD we have

$$\begin{aligned} I_{ac} &= \frac{\Re G [|E_1|^2 + |E_2|^2]}{2} \\ &= \left\{ \begin{array}{l} \Gamma_1 [\cos(\Omega_1 t) + \cos(\Omega_2 t)] \\ +\Gamma_2 [\cos(2\Omega_1 - \Omega_2)t + \cos(2\Omega_2 - \Omega_1)t] \end{array} \right\} \end{aligned} \quad (9)$$

$$E_2(t) = E_{c2} e^{j\omega_c t} \left\{ \begin{array}{l} \cos\left(\frac{\phi}{2}\right) \left\{ \begin{array}{l} \sqrt{a} J_{+1} J_{-1} \{e^{j(\Omega_2 - \Omega_1)t} + e^{j(\Omega_1 - \Omega_2)t}\} \\ +\sqrt{a} J_0 J_0 \end{array} \right\} \\ -\sin\left(\frac{\phi}{2}\right) \left\{ \begin{array}{l} J_{+1} J_0 [e^{j\Omega_2 t} + e^{j\Omega_1 t}] \\ +J_{+2} J_{-1} \{e^{j(2\Omega_1 - \Omega_2)t} + e^{j(2\Omega_2 - \Omega_1)t}\} \end{array} \right\} \\ -\cos\left(\frac{\phi}{2}\right) \left\{ \begin{array}{l} J_{+2} J_0 [e^{j2\Omega_2 t} + e^{j2\Omega_1 t}] \\ +J_{+1} J_{+1} e^{j(\Omega_2 + \Omega_1)t} \end{array} \right\} \end{array} \right\} \quad (7)$$

$$I_{ac2} = \frac{\Re|E_2|^2}{2} \approx P_{in2} \Re \left\{ \sin(\phi) \left\{ \begin{array}{l} \begin{bmatrix} J_{+1} J_0^2 J_{+2} + J_{+1}^3 J_0 \\ -\sqrt{a} J_0^3 J_{+1} + \sqrt{a} J_{+1}^3 J_0 \end{bmatrix} \begin{bmatrix} \cos(\Omega_1 t) \\ +\cos(\Omega_2 t) \end{bmatrix} \\ + \begin{bmatrix} J_{+1} J_0^2 J_{+2} \\ \sqrt{a} J_0^2 J_{+2} J_{+1} \\ +\sqrt{a} J_{+1}^3 J_0 \end{bmatrix} \begin{bmatrix} \cos((2\Omega - \Omega_2)t) \\ +\cos((2\Omega_2 - \Omega_1)t) \end{bmatrix} \end{array} \right\} \right\} \quad (8)$$

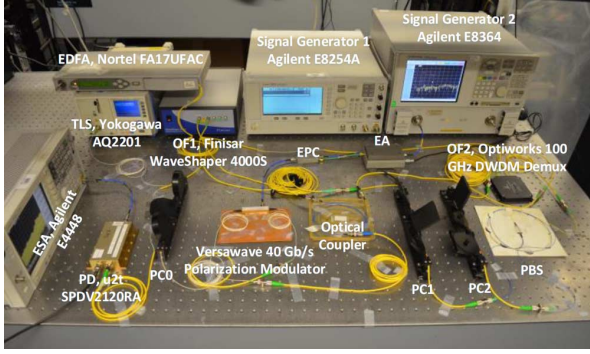


Fig. 2. Photograph showing the experiment setup of the proposed MPL. Electrical amplifier: EA, erbium-doped fiber amplifier: EDFA, electrical power combiner: EPC, electrical spectrum analyzer: ESA, optical filter: OF, photodetector: PD, polarization controller: PC, polarization beam splitter: PBS, tunable laser source: TLS.

where G is the gain of the EDFA, and the coefficients for the fundamental and IMD3 components are, Γ_1 and Γ_2 , respectively. When $\beta \leq 1$, $J_{+1}J_{+1} \approx 2J_{+2}J_0$, Γ_1 , and Γ_2 can be simplified and given by

$$\begin{aligned} \Gamma_1 &= \Re G \left[\begin{array}{l} P_{in2} \sin(\phi) (-\sqrt{a} J_0^3 J_{+1} + (3 + 2\sqrt{a}) J_{+1} J_0^2 J_{+2}) \\ -3P_{in1} J_{+1} J_0^2 J_{+2} \end{array} \right] \\ \Gamma_2 &= \Re G \left[P_{in2} \sin(\phi) (1 + 3\sqrt{a}) J_{+1} J_0^2 J_{+2} - P_{in1} J_{+1} J_0^2 J_{+2} \right]. \end{aligned} \quad (10)$$

To increase the SFDR of the proposed MPL, the IMD3 terms have to be fully cancelled. Therefore, Γ_2 should be zero, which leads to

$$\frac{P_{in1}}{P_{in2}} = \sin(\phi) (1 + 3\sqrt{a}). \quad (11)$$

As can be seen from (11), P_{in1}/P_{in2} can be various values for various ϕ and \sqrt{a} , and an optimal choice for the ratio of P_{in1} to P_{in2} is to maximize the SFDR while fully canceling the IMD3 terms. According to [15] and [16], for a constant optical power sent to a PD, when the carrier-to-sideband ratio (CSR) is 0 dB for the lower channel, the SFDR will be optimized. The optical carrier suppression is realized by low biasing the equivalent MZM. The values for the parameters in (11) to have an optimized dynamic range are given by

$$\phi = \frac{8\pi}{9} \quad a = -4 \text{ dB} \quad \frac{P_{in1}}{P_{in2}} = 0.9894 \approx 1. \quad (12)$$

Here, we assume that the first-order sidebands having a power that is around 20 dB lower than that of the optical carrier when the MZM is biased at the quadrature point for linear operation.

III. EXPERIMENTAL RESULTS

To verify that the proposed MPL is effective in the improvement of the SFDR, a proof-of-concept experiment based on the setup shown in Fig. 2 is conducted. A continuous-wave (CW) light at 1545.284 nm from a tunable laser source (TLS, Yokogawa AQ2201) is sent to a PolM (Versawave) via PC0. The polarization direction of the light wave incident to the PolM is adjusted by PC0 to have an angle of 45° relative to one principal axis of the PolM. The half-wave voltage and the bandwidth of

the PolM are 3.5 V and 40 GHz, respectively. The two complementarily modulated light waves along the two principal axes of the PolM are then sent to a 3-dB coupler. The lengths of the upper and lower channels are controlled to be identical. In the upper channel, an OF (Finisar WaveShaper 4000S) is incorporated to suppress the optical carrier and all the lower order sidebands. The power suppression ratio is around 40 dB. Note that PC1 is tuned to make the static phase term introduced by PC1 be equal to $-\pi/2$, thus the equivalent MZM in the upper channel is biased at the quadrature point. In the lower channel, an OF (one channel of a WDM, Optiworks 100 GHz DWDM Demux) is used to select the upper sidebands, partially suppress the optical carrier, and fully filter out the lower sidebands. The power suppression ratios for the optical carrier and lower sidebands are 4 dB [the optimal value given in (12)] and 23.06 dB, respectively. The static phase term introduced by PC2 is adjusted to be approximately $8\pi/9$, again an optimal value in (12). Thus, the optical carrier is suppressed by low biasing the equivalent MZM (Ch2). The optical suppression ratio is around 15 dB. Finally, the optical signals from the two channels are combined at the PBS and then amplified to 9.45 dBm before being applied to the PD (u^2t , SPDV2120RA). The responsivity and the bandwidth of the PD is 0.65 A/W and 50 GHz, respectively.

The performance for the proposed MPL and the performance comparison with a conventional PolM-based intensity modulated MPL [shown in Fig. 1(b)] are performed based on a two-tone test. First, we measure the spectra of the RF signals at the output of the PD and the carrier-to-interference ratios (CIRs) for both the proposed MPL and the conventional PolM-based intensity modulated MPL. Two RF signals at 18.70 and 18.71 GHz with an identical power are generated by a network analyzer (Agilent E8364) and a signal generator (Agilent E8254A), respectively, and then are combined and applied to the PolM via the RF electrode. The power for each of the two input RF signals is set at -2 dBm. The electrical spectra of the detected RF signals at the output of the PD are measured by an electrical spectrum analyzer (ESA) (Agilent E4448). Fig. 3(a) shows the electrical spectrum obtained at the output of the PD for the conventional PolM-based MPL (note that the power for each of the two input RF signals is -2 dBm). As can be seen, strong IMD3 components are observed. The CIR is 42.011 dB. Fig. 3(b) shows the electrical spectrum at the output of the PD for the proposed MPL (note that the power for each of the two input RF signals is -2 dBm). As can be seen, a CIR of more than 68.465 dB is achieved. The improvement of the CIR is 26.454 dB.

The SFDR performance is then measured. Fig. 4(a) shows the experimental results for the conventional PolM-based MPL. The SFDR is $90.34 \text{ dB} \cdot \text{Hz}^{2/3}$ for a noise floor of -140 dBm/Hz . Fig. 4(b) shows the experimental results for the proposed MPL. The SFDR is $106.16 \text{ dB} \cdot \text{Hz}^{2/3}$ for a noise floor of -140 dBm/Hz . As can be seen, the improvement of the SFDR is 15 dB. In the experiment, the noise floor of -140 dBm/Hz is limited by the ESA used. Usually, in an MPL with an optical power of a few dBm, the largest contribution to the output noise is the shot noise. Here, if we assume that the proposed MPL is a shot noise limited link, the noise floor can be -166 dBm/Hz . The SFDR of the proposed MPL is then

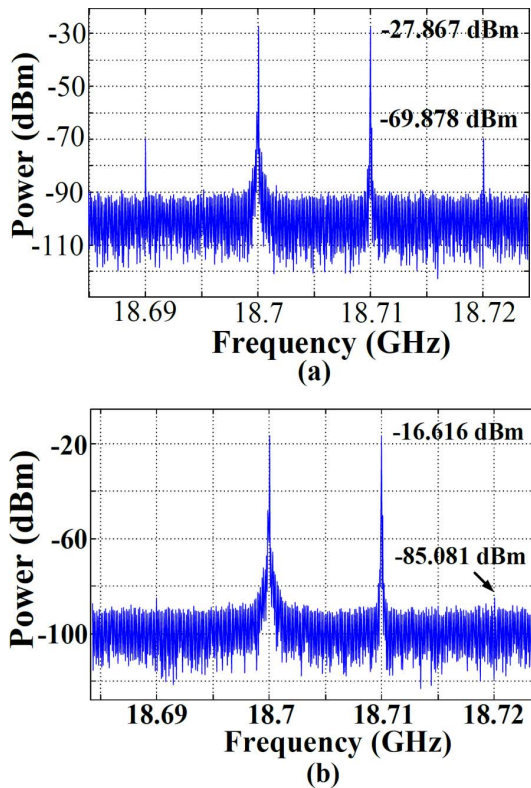


Fig. 3. Electrical spectra of the detected RF signals at the output of the PD when a two-tone RF signal is applied to the PolM. (a) Conventional PolM-based MPL. (b) Proposed MPL, RBW: 7.5 kHz.

123.48 dB · Hz^{2/3}. In [10], if the optical power sent to the PD is also 9.45 dBm, the SFDR can be 116.33 dB · Hz^{2/3} for a noise floor of -166 dBm/Hz, which is 7.15 dB poorer than that of the proposed MPL. This confirms that the joint use of the two techniques will further improve the dynamic range.

IV. DISCUSSIONS

The bias points of the equivalent MZMs for both the upper and lower channels depend on the polarization direction of the lightwave entering the PolM, the polarization directions of the lightwaves entering the PBS, and the static phase terms introduced by the two PCs (PC1 and PC2) in the two channels. For real implementation, the polarization directions can be controlled precisely if polarization-maintaining fibers are employed. Here, we discuss the dependence of the SFDR on the static phase terms introduced by the PCs, which will affect the bias points of the equivalent MZMs. For channel 1, after the OF, since the main portion of the lightwave (the optical carrier) is filtered out, a change to the static phase, or equivalently, the bias point of the equivalent MZM (Ch1) will not have a significant impact on the SFDR. While for channel 2, if the static phase introduced by PC2 is changed, the power of the optical carrier will change significantly, which would lead to a large change to the SFDR. Fig. 5 shows a numerical simulation in which the SFDR for the equivalent MZM (Ch2) operating at different bias points due to the change of the static phase introduced by PC2 is calculated. As can be seen when the static phase is $8\pi/9 \approx 2.79$, a largest SFDR is achieved. When the

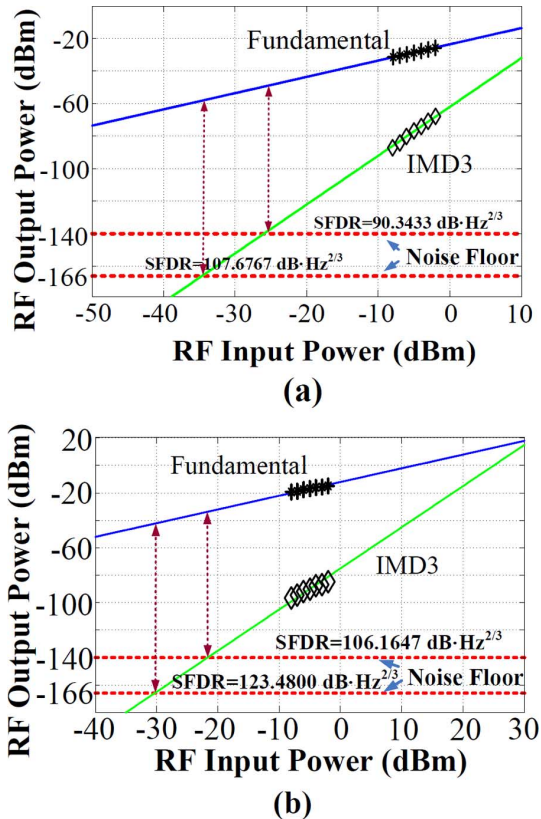


Fig. 4. Measured RF powers of the fundamental and the IMD3 terms at the output of the PD when a two-tone signal is applied to the PolM. (a) Conventional PolM-based MPL. (b) Proposed MPL.

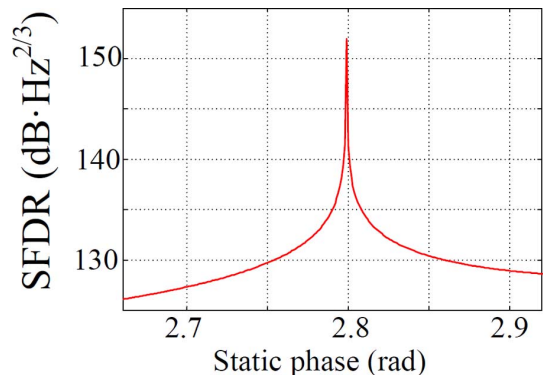


Fig. 5. SFDR of the proposed MPL for the equivalent MZM (Ch2) operating at a different bias point due to the change of the static phase introduced by PC2.

static phase term is drifting away from 2.79, the SFDR will decrease significantly. The phase drift can be eliminated if a waveplate is employed to replace the PC.

In the experiment, we used a Finisar WaveShaper 4000S and one channel of an Optiworks 100-GHz DWDM Demux (four channels total) as the two OFs in the proposed MPL. The bandwidth of the MPL, especially the lower cutoff frequency, was limited by the poor steepness of the band edges and the poor out-of-band rejection of the two OFs. However, in a practical system, the steepness of the band edges and the out-of-band rejection can be improved, such as the use of two sharp-edge wide-band fiber Bragg gratings, as reported recently in [17], then the bandwidth of the MPL can be very large.

V. CONCLUSION

We have proposed and experimentally demonstrated a novel MPL with an improved SFDR using a single PolM. The suppression of IMD3 terms was achieved by destructive combination of the distortion signals in the electrical domain. Using two OFs to filter out the optical carrier and its lower sidebands of one channel and the lower sidebands of another channel, we could make the IMD3 terms be completely suppressed when the optical powers into the two channels were controlled identical. In addition, due to the partial suppression of the optical carrier via low biasing in the lower channel while maintaining an identical optical power, the modulation efficiency of the equivalent MZM in the lower channel was increased, which led to an increase in the gain of the MPL. Thus, the SFDR of the MPL was further increased. The performance of the proposed MPL was experimentally evaluated. Compared with a conventional PolM-based intensity-modulation-based MPL, an improvement in SFDR of 15 dB was achieved, which was 7.15 dB more than that of the MPL using two optical paths to produce two identical, but complementary IMD3 terms reported by us in [10].

REFERENCES

- [1] C. Cox, *Analog Optical Links: Theory and Practice*. Cambridge, U.K.: Cambridge Univ. Press, 2004.
- [2] L. T. Nichols, K. J. Williams, and R. D. Esman, "Optimizing the ultrawide-band photonic link," *IEEE Trans. Microw. Theory Techn.*, vol. 45, no. 8, pp. 1384–1389, Aug. 1997.
- [3] B. Hraimel and X. Zhang, "Low-cost broadband predistortion-linearized single-drive x-cut Mach-Zehnder modulator for radio-over-fiber system," *IEEE Photon. Technol. Lett.*, vol. 24, no. 18, pp. 1571–1573, Sep. 2012.
- [4] Q. Lin, Z. Z. Ying, and G. Wei, "Design of a feedback predistortion linear power amplifier," *Microw. J.*, vol. 48, no. 5, pp. 232–241, May 2005.
- [5] M. L. Farwell, W. S. C. Chang, and D. R. Huber, "Increased linear dynamic range by low biasing the Mach-Zehnder modulator," *IEEE Photon. Technol. Lett.*, vol. 5, no. 7, pp. 779–782, Jul. 1993.
- [6] E. I. Ackerman, "Broadband linearization of a Mach-Zehnder electro-optic modulator," *IEEE Trans. Microw. Theory Techn.*, vol. 47, no. 12, pp. 2271–2279, Dec. 1999.
- [7] M. Huang, J. Fu, and S. Pan, "Linearized analog photonic links based on a dual-parallel polarization modulator," *Opt. Lett.*, vol. 37, no. 11, pp. 1823–1825, Jun. 2012.
- [8] S. K. Korotky and R. M. DeRidder, "Dual parallel modulation schemes for low-distortion analog optical transmission," *IEEE J. Sel. Areas Commun.*, vol. 8, no. 1, pp. 1377–1381, Sep. 1990.
- [9] J. Dai *et al.*, "Optical linearization for intensity-modulated analog links employing equivalent incoherent combination technique," in *Proc. MWP*, Oct. 2011, pp. 230–233.
- [10] X. Chen, W. Li, and J. P. Yao, "Microwave photonic link with improved dynamic range using a polarization modulator," *IEEE Photon. Technol. Lett.*, vol. 25, no. 14, pp. 1373–1376, Jul. 2013.
- [11] W. Li and J. P. Yao, "Spurious-free dynamic range improvement of a microwave photonic link based on bi-directional use of a polarization modulator in a Sagnac loop," *Opt. Exp.*, vol. 21, no. 13, pp. 15692–15697, Jul. 2013.
- [12] W. Li and J. P. Yao, "Microwave and terahertz generation based photonically assisted microwave frequency twelvetyupling with large tenability," *IEEE Photon. J.*, vol. 2, no. 6, pp. 954–959, Dec. 2010.
- [13] S. Pan and J. P. Yao, "A frequency-doubling optoelectronic oscillator using a polarization modulator," *IEEE Photon. Technol. Lett.*, vol. 21, no. 13, pp. 929–931, Jul. 2009.
- [14] Y. Cui *et al.*, "Intermodulation distortion suppression for intensity-modulated analog fiber-optic link incorporating optical carrier band processing," *Opt. Exp.*, vol. 21, no. 20, pp. 23 433–23 440, Oct. 2013.

- [15] C. Lim, M. Attygalle, A. Nirmalathas, D. Novak, and R. Waterhouse, "Analysis of optical carrier-to-sideband ratio for improving transmission performance in fiber-radio links," *IEEE Trans. Microw. Theory Techn.*, vol. 54, no. 5, pp. 2181–2186, May 2006.
- [16] M. J. LaGasse, W. Charczenko, M. C. Hamilton, and S. Thaniyavarn, "Optical carrier filtering for high dynamic range fibre optic links," *Electron. Lett.*, vol. 30, no. 25, pp. 2157–2158, Dec. 1994.
- [17] X. Zou, M. Li, L. Yan, J. Azana, and J. P. Yao, "All-fiber optical filter with an ultra-narrow and rectangular spectral response," *Opt. Lett.*, vol. 38, no. 18, pp. 3096–3098, Aug. 2013.

Xiang Chen (S'13) received the B.Eng. degree in communications engineering from Donghua University, Shanghai, China, in 2009, the M.Sc. degree in communications and information engineering from Shanghai University, Shanghai, China, in 2012, and is currently working toward the Ph.D. degree in electrical and computer engineering at the Microwave Photonics Research Laboratory, School of Electrical Engineering and Computer Science, University of Ottawa, Ottawa, ON, Canada.

His current research interests include coherent radio-over-fiber systems and analog optical links.

Wangzhe Li (GSM'09–M'13) received the B.E. degree in electronic science and technology from Xi'an Jiaotong University, Xi'an, China, in 2004, the M.Sc. degree in optoelectronics and electronic science from Tsinghua University, Beijing, China, in 2007, and the Ph.D. degree in electrical engineering from the University of Ottawa, Ottawa, ON, Canada, in 2013.

He is currently a Postdoctoral Fellow with the Microwave Photonics Research Laboratory, School of Electrical Engineering and Computer Science, University of Ottawa. His current research interests include photonic generation of microwave and terahertz signals, arbitrary waveform generation, opto-electronic oscillation, and silicon photonics.

Dr. Li was a recipient of a 2011 IEEE Microwave Theory and Techniques Society (IEEE MTT-S) Graduate Fellowship and a 2011 IEEE Photonics Society Graduate Fellowship.

Jianping Yao (M'99–SM'01–F'12) received the Ph.D. degree in electrical engineering from the Université de Toulon, Toulon, France, in 1997.

He is currently a Professor and University Research Chair with the School of Electrical Engineering and Computer Science, University of Ottawa, Ottawa, ON, Canada. In 1998, he joined the School of Electrical and Electronic Engineering, Nanyang Technological University, Singapore, as an Assistant Professor. In December 2001, he joined the School of Electrical Engineering and Computer Science, University of Ottawa, as an Assistant Professor, where he became an Associate Professor in 2003, and a Full Professor in 2006. He was appointed University Research Chair in Microwave Photonics in 2007. From July 2007 to June 2010, he was the Director of the Ottawa–Carleton Institute for Electrical and Computer Engineering. In 2013, he was re-appointed Director of the Ottawa–Carleton Institute for Electrical and Computer Engineering. He has authored or coauthored more than 460 papers, including more than 260 in peer-reviewed journals and 200 in conference proceedings.

Dr. Yao is a registered Professional Engineer in the Province of Ontario. He is a Fellow of the Optical Society of America (OSA) and the Canadian Academy of Engineering. He was a guest editor for the "Focus Issue on Microwave Photonics" in *Optics Express* in 2013 and a "Feature Issue on Microwave Photonics" in *Photonics Research* in 2014. He is currently a topical editor for *Optics Letters*. He serves on the Editorial Board of the IEEE TRANSACTIONS ON MICROWAVE THEORY AND TECHNIQUES, *Optics Communications*, and *China Science Bulletin*. He is a chair of numerous international conferences, symposia, and workshops, including the Vice Technical Program Committee (TPC) chair of the IEEE Microwave Photonics Conference in 2007, TPC co-chair of the Asia-Pacific Microwave Photonics Conference in 2009 and 2010, TPC chair of the High-Speed and Broadband Wireless Technologies Subcommittee of the IEEE Radio Wireless Symposium in 2009–2012, TPC chair of the Microwave Photonics Subcommittee of the IEEE Photonics Society Annual Meeting in 2009, TPC chair of the IEEE Microwave Photonics Conference in 2010, General co-chair of the IEEE Microwave Photonics Conference in 2011, TPC co-chair of the IEEE Microwave Photonics Conference in 2014, and general co-chair of the IEEE Microwave Photonics Conference in 2015. He is an IEEE Microwave Theory and Techniques Society (IEEE MTT-S) Distinguished Microwave Lecturer for 2013–2015. He was the recipient of the 2005 International Creative Research Award of the University of Ottawa, the 2007 George S. Glinski Award for Excellence in Research, and the inaugural OSA outstanding reviewer award in 2012.